A photoactive carotenoid protein acting as light intensity sensor

Adjélé Wilson*, Claire Punginelli*, Andrew Gall*, Cosimo Bonetti†, Maxime Alexandre†, Jean-Marc Routaboul‡, Cheryl A. Kerfeld§, Rienk van Grondelle†, Bruno Robert*, John T. M. Kennis†, and Diana Kirilovsky*¶

*Commissariat à l'Energie Atomique, Institut de Biologie et Technologies de Saclay and Centre National de la Recherche Scientifique, 91191 Gif sur Yvette, France; †Department of Physics and Astronomy, Faculty of Sciences, VU University Amsterdam, De Boelelaan 1081 HV Amsterdam, The Netherlands; ‡Laboratoire de Biologie des Semences, Institut National de la Recherche Agronomique-AgroParisTech, Institut Jean-Pierre Bourgin, 78026 Versailles, France; and §Joint Genome Institute, United States Department of Energy, Walnut Creek CA 94598 andDepartment of Plant and Microbial Biology, University of California, Berkeley, CA 94720

Edited by Robert Haselkorn, University of Chicago, Chicago, IL, and approved June 6, 2008 (received for review May 16, 2008)

Intense sunlight is dangerous for photosynthetic organisms. Cyanobacteria, like plants, protect themselves from light-induced stress by dissipating excess absorbed energy as heat. Recently, it was discovered that a soluble orange carotenoid protein, the OCP, is essential for this photoprotective mechanism. Here we show that the OCP is also a member of the family of photoactive proteins; it is a unique example of a photoactive protein containing a carotenoid as the photoresponsive chromophore. Upon illumination with blue-green light, the OCP undergoes a reversible transformation from its dark stable orange form to a red "active" form. The red form is essential for the induction of the photoprotective mechanism. The illumination induces structural changes affecting both the carotenoid and the protein. Thus, the OCP is a photoactive protein that senses light intensity and triggers photoprotection.

cyanobacteria | nonphotochemical quenching | photoprotection | phycobilisome

To maximize the use of sunlight, photosynthetic organisms collect as much light as possible using an antenna made up of pigments attached to special proteins. However, excess light is harmful because it can induce the formation of dangerous oxygen species in the photochemical reaction centers. Under full sunlight conditions, a safety valve must be opened to convert the excess into heat and to reduce the amount of energy funneled to reaction centers. It is well known that in plants carotenoids play an essential role in photoprotective mechanisms within the chlorophyll-membrane antenna of photosystem II (PSII) (1–7). In contrast, the mechanism of thermal energy dissipation in cyanobacteria, which plays a key role in global carbon cycling, remained elusive. Only within the last few years has a photoprotective mechanism associated with the soluble phycobilisome antenna of PSII in cyanobacteria been demonstrated (8–14). A specific soluble carotenoid protein, the orange carotenoid protein (OCP), plays an essential role in this process (9, 10). In its absence, thermal dissipation is abolished, rendering the cells more sensitive to high light intensities; this is manifested as a faster decrease in PSII activity in a mutant lacking the OCP (9). Surprisingly, the role of the carotenoid in the OCP is completely different from the role of the photoprotective carotenoids in plants. The OCP appears to act as a photoreceptor, responding to blue-green light; this induces energy dissipation, resulting in a detectable quenching of the cellular fluorescence, known as nonphotochemical-quenching (NPQ), through interaction with the phycobilisome (9, 11). In mutants containing the OCP but lacking phycobilisomes, blue-green light was unable to induce the photoprotective mechanism (9, 10).

The OCP, a 35 kDa protein that contains a single noncovalently bound carotenoid (15–18), is the product of the *slr1963* gene in *Synechocystis* PCC 6803 (16). Highly conserved homologs of the OCP are found in most of the cyanobacterial genomes. The structure of the *Arthrospira maxima* OCP has been determined to 2.1 Å resolution (19). It consists of two domains: a unique α-helical N-terminal domain and a mixed α-helical/β-sheet C-terminal domain. The embedded keto carotenoid, 3′-hydroxyechinenone (hECN), composed of a conjugated carbonyl group located at the terminus of a conjugated chain of 11 carbon-carbon double bonds in an all-trans configuration. The carotenoid spans both protein domains with its keto terminus nestled within the C-terminal mixed α/β domain. Absolutely conserved Tyr-44 and Trp-110 make hydrophobic contacts with the hydroxyl terminal end of the carotenoid, whereas two other absolutely conserved residues, Tyr-203 and Trp-290, form hydrogen bonds to the carbonyl moiety at the keto terminus of the pigment (19) (refer also to Fig. 3*A*).

Results

To isolate the OCP, C-terminal His-tagged OCP mutants were constructed in *Synechocystis* PCC 6803, using kanamycin or spectinomycin resistance for mutant selection [supporting information (SI) Figs. S1 and S2]. In the WT and the kanamycin resistant mutant, blue-green light induced similar fluorescence quenching, indicating that the presence of the His-tag did not affect the activity of the OCP. In the spectinomycin resistant mutant, the fluorescence quenching was slightly decreased relative to the WT (Fig. 1*A*); this correlates with a lower concentration of the OCP in this mutant (probably because of a destabilization of the mRNA) (Fig. 1*B*). In addition, a mutant was constructed in which the *slr1963* gene containing a C-terminal His-tag was expressed using the *psbA2* promoter region as the promoter. In this strain, large quantities of the OCP were present (see Fig. 1*B*) and a very large fluorescence quenching was observed (see Fig. 1*A*), confirming the relationship between OCP concentration and excitation energy quenching. The OCP was isolated using affinity Ni-chromatography followed by an ion-exchange column (Fig. S3). The absorption spectrum of the His-tagged OCP isolated from *Synechocystis* 6803 is essentially identical to that of *A. maxima* (compare Fig. 2*B* dark form with the spectrum in Fig. 2 in ref. 20). As in the latter strain, it mainly binds hECN (Fig. S4).

In darkness or dim light the OCP appears orange (OCP^o) and its absorption spectrum presents a typical carotenoid shape, reflecting the strongly allowed S_0-S_2 transition with three distinct vibrational bands; the 0–0 vibrational peak is located at 496 nm

Author contributions: R.v.G., B.R., J.T.M.K., and D.K. designed research; A.W., C.P., A.G., C.B., M.A., J.-M.R., and D.K. performed research; A.W., C.P., A.G., J.-M.R., and D.K. analyzed data; and C.A.K., B.R., J.T.M.K., and D.K. wrote the paper.

The authors declare no conflict of interest.

This article is a PNAS Direct Submission.

¶To whom correspondence should be addressed at: Institut de Biologie et Technologies de Saclay, Bât 532, Commissariat à l'Energie Atomique Saclay, 91191 Gif sur Yvette, France. E-mail: diana.kirilovsky@cea.fr.

This article contains supporting information online at www.pnas.org/cgi/content/full/0804636105/DCSupplemental.

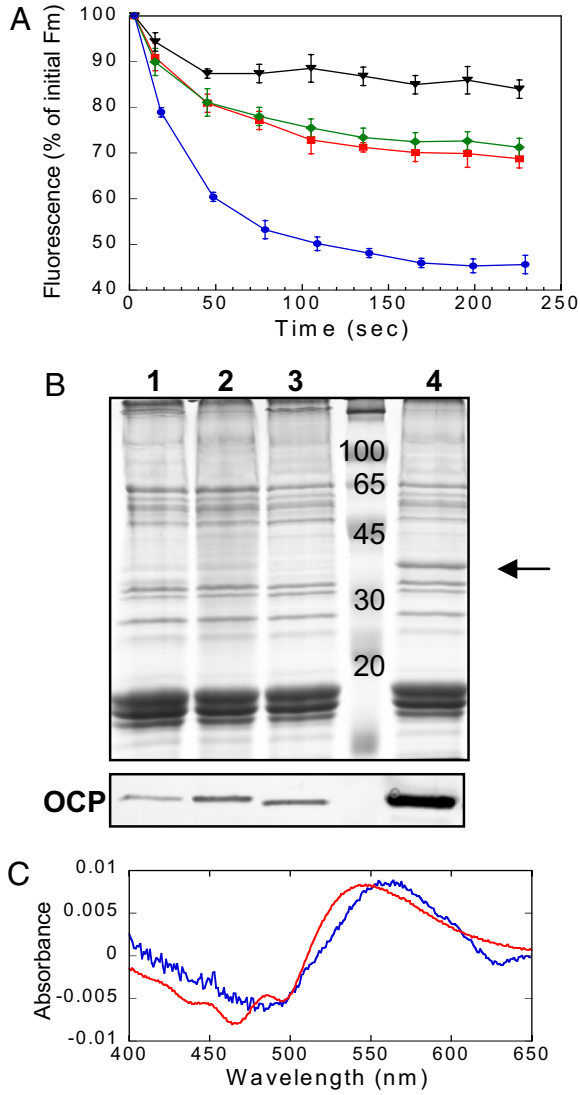

Fig. 1. Relationship between blue-green light induced NPQ and the OCP in whole cells. (*A*) Decrease of maximal fluorescence (Fm′) during exposure of WT (*red squares*), over-expressing OCP mutant (*blue circles*), His-tagged OCP/K_m resistant mutant (*green romboids*) and His-tagged OCP/Sp resistant mutant (*black triangles*) cells to 740-μmol photons m^{-2} s^{-1} of blue-green light (400–550 nm). The graph is the average of four independent experiments and the error bars show the maximum and the minimum fluorescence value for each point. The cells were diluted to 3-μg chlorophyll/ml. (*B*) Coomassie blue-stained gel electrophoresis and immunoblot detection (*bottom panel*) in membrane-phycobilisome fractions from His-tagged OCP/Sp resistant mutant (*1*), His-tagged OCP/K_m resistant mutant (*2*), WT (*3*), and over-expressing OCP mutant (*4*). The arrow indicates the OCP. Each lane contained 1.5-μg chlorophyll. (*C*) OCP^r is present in whole cells under NPQ-inducing conditions. Difference light-minus-dark absorbance spectrum of the isolated OCP (*red*) compared with the double difference absorbance spectrum: light-minus-dark overexpressing OCP cells spectrum minus light-minus-dark ΔOCP cells [strain without OCP (9)] (average of five independent experiments). The illumination of cells and spectra recording were realized at 11°C.

(see Fig. 2 *A* and *B*). The position and shape of this transition corresponds to that of hECN locked into an all-trans conformation by the surrounding protein (20), in agreement with the crystallographic structure (19). Strikingly, upon illumination with blue-green light (400–550 nm) at 10°C, the OCP^o is completely photoconverted to a red form, OCP^r. The red-shifted spectrum of OCP^r with a maximum at 500 nm loses the resolution of the vibrational bands (see Fig. 2 *A* and *B*). To elucidate whether the conversion of the OCP^o to OCP^r occurs in whole cells under NPQ-inducing conditions, absorbance spectra of whole cells of the overexpressing OCP strain and the ΔOCP strain, lacking the OCP (9), were measured before and after illumination with high intensities of blue light at 11°C and the light-minus-dark difference spectra calculated. Our results strongly suggested that OCP^r is accumulated *in vivo* under the conditions inducing energy dissipation and fluorescence quenching (Fig. 1*C*).

In darkness, OCP^r spontaneously reverts to the orange form (Fig. 2*C*). This step is not accelerated by illumination (Fig. S5). The back-reaction kinetics (red to orange) shows a large temperature dependence, the half-time of recovery varying from 30 sec at 32°C to ≈45 min at 11°C. *In vivo*, the recovery NPQ kinetics also show a large temperature dependence; however, the kinetics are slower (8, 9, 14) than the OCP^r to OCP^o dark conversion, suggesting that the OCP^r form is more stable *in vivo* than *in vitro* or that the fluorescence quenching remains longer than the OCP^r form. In contrast, the initial rate of the light photoconversion was temperature-independent (Fig. 2*D*). Thus, at a fixed light intensity, the steady-state concentration of OCP^r depended on the temperature. This is reflected *in vivo*, where a larger NPQ was observed at 7°C than at 33°C (Fig. S6). The kinetics of OCP^r formation strongly depended on light intensity (Fig. 2*E*). This correlates with the observed dependency on light intensity of the blue-light induced NPQ in whole cells (9).

Collectively, these results strongly suggested that OCP^r is the active form of the OCP and that pigment-protein interactions are critical to this activity. To confirm this, a C-terminal His-tagged W110S-OCP mutant and an overexpressing C-terminal His-tagged W110S OCP mutant were constructed and characterized. High intensities of blue-green light induced no fluorescence quenching in the mutant (Fig. 3*B*), indicating that Trp-110 is critical to the OCPs photoprotective function. This was substantiated by construction of an overexpressing W110S-OCP mutant in which very little quenching was induced, although large quantities of OCP were present (see Fig. 3 *B* and *C*). The absorbance spectrum of the isolated mutated OCP was similar to that of the WT OCP (Fig. 3*D*). Moreover, each isolated mutant OCP contains a carotenoid molecule as judged by comparison to WT OCP (similar A_{467}/A_{280} ratio, data not shown). High intensities of blue-green light converted only a very small portion of the OCP^o to OCP^r, even after 15 min of illumination at 10°C (see Fig. 3*D*). Thus, there is a direct correlation between the accumulation of OCP^r and the induction of the fluorescence quenching.

Resonance Raman spectroscopy was used to observe light-induced structural changes of the hECN. The Raman spectra of the OCP^o from *A. maxima* and *Synechocystis* PCC 6803 are nearly identical, indicating that the carotenoid-peptide interactions in these two proteins are remarkably homologous (Fig. 4*A*). Thus, the X-ray structure from the former strain may be used as a model for the OCP of the latter. This has been confirmed by the determination of the 1.65 Å structure of the *Synechocystis* PCC6803 OCP (C.A.K., unpublished results). Before illumination, the resonance Raman spectra of OCP-bound hECN shows that this carotenoid is in an all-trans conformation, in good agreement with the X-ray structure (19). The relatively high intensity of the bands in the ν_4 region, however, indicates that this conformation is not planar, but highly distorted around the C-C bonds (21). Upon illumination the position of C = C stretching mode shifts from 1,528 cm^{-1} to 1,521 cm^{-1}, indicating that the apparent conjugation length of hECN increased by about one conjugated bond (22), in agreement with the observed red-shift (see Fig. 4*A*). Trans-*cis* isomerisation of hECN should shift down the position of this band, and should result in the appearance of new bands in the spectra because of the change in the molecular symmetry. As this is not observed, we can conclude that hECN is still all-trans in its red form. Of course,

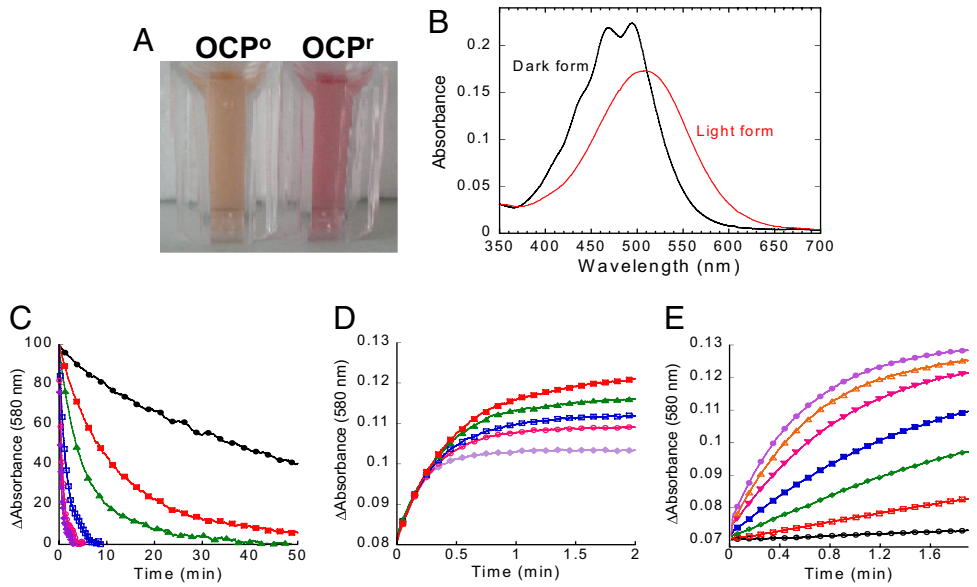

Fig. 2. Isolated OCP is responsive to blue-green light: Photoconversion and dark recovery. (*A*) Photograph of isolated OCP^o and OCP^r. To obtain OCP^r the isolated protein was illuminated with a blue-green light at 740-μmol photons m^{-2} s^{-1} at 12°C for 2 min. (*B*) Absorbance spectra of the dark orange form (OCP^o; black) and the light red form (OCP^r; red). (*C*) Darkness red OCP^r to orange OCP^o conversion (decrease of the absorbance at 580 nm) and (*D*) photoconversion from the OCP^o to the OCP^r form using a 350-μmol photon m^{-2} s^{-1} blue-green light intensity (increase of the absorbance at 580 nm) at different temperatures: 32°C (violet), 28°C (rose), 24°C (blue), 19°C (green), 15°C (red), and 11°C (black). (*E*) OCP^r accumulation at 11°C and different light intensities: 20 (black), 50 (red), 120 (green), 210 (blue), 350 (rose), 740 (orange), and 1,200 (violet)-μmol photons m^{-2} s^{-1} of blue-green (400–550 nm). The protein concentration was OD 0.2 at 495 nm.

we cannot formally discard presence of end chain isomerisation (such as 7-*cis*), whose effect on the Raman spectra (and on the electronic absorption spectra) is limited. The decrease of intensity of the 950 cm^{-1} indicates that upon photoconversion, hECN reaches a less distorted, more planar structure (22). Similar differences were observed using the OCP from *A. maxima* (data not shown). Further studies will be necessary to elucidate the specific nature of the changes in the carotenoid.

Light-induced Fourier transform infrared (FTIR) difference spectroscopy was applied to probe the light-induced structural changes in the protein of the OCP. Upon illumination, large changes in the OCP FTIR spectra can be observed ≈1,650 and 1550 cm^{-1}, where the Amide I and Amide II protein modes are expected to contribute. In the light-minus-dark FTIR spectra, these protein contributions, with specific frequencies for each type of protein secondary structure (loops, α-helix, and β-sheet) (23), may be formally attributed to the protein modes on the basis of their sensitivity to D_2O exchange (hECN molecules contain only one, nonconjugated, exchangeable proton) (Fig. 4*B*). The differential signal at 1,677(−)/1,697(+) cm^{-1} is assigned to portions of the protein without secondary structure: that is, the loops. The α-helix and β-sheet carbonyl region shows an intense and broad negative band centered at 1,643 cm^{-1}, which has a corresponding induced absorption at 1,663(+) and 1,618(+)cm^{-1} assigned to α-helix and β-sheet, respectively. Light-induced Amide I changes in the OCP are large, suggesting a major rearrangement of the protein backbone. An up-shift of the Amide I vibrations of α-helix corresponds to a weakening of the NH − C = O hydrogen bonds that connect the turns, indicating a less rigid helical structure in a significant part of OCP upon formation of the red form. A down-shift of the Amide I vibrations of β-sheet corresponds to a shortening (ie, a strengthening) of the NH − C = O H-bonds between the β strands, resulting in a compaction of the β-sheet domain upon formation of the red form. The Amide I frequency-shift pattern observed here for OCP is strikingly similar to that observed in the LOV2 domain of phototropin, a flavin-binding blue-light photoreceptor (24).

Ultrafast spectroscopy was applied to examine the primary photochemistry of the OCP and the efficiency of product formation. Fig. 5*A* shows the result of a global analysis of the time-resolved data. Four kinetic components are required for an adequate fit. The 100-fs component corresponds to internal conversion of the initially excited, optically allowed, S_2 state of the carotenoid to the low-lying, optically forbidden S_1 state coupled to an intramolecular charge-transfer (ICT) state. The 1-ps and 4.5-ps components correspond to decay of the S_1 and ICT states, respectively (20). After decay of the hECN excited states on a ps timescale, a photoproduct remains at very low amplitude (Fig. 5*B*). The spectral signature of this product species is similar to that of the light-minus-dark spectrum of the OCP (see Fig. 5*A*). However, the primary product is slightly red-shifted with respect to that of the light-minus-dark, indicating that these states may be similar but not identical and that relaxation takes place on timescales longer than nanoseconds. The amplitude of the product state at 565 nm is only 1% of that of the original carotenoid bleach near 475 nm immediately after excitation (see Fig. 5*A*), consistent with the assumption that the OCP is a low quantum-yield photoactive protein.

Discussion

Previously, we demonstrated that the OCP is specifically involved in a photoprotective phycobilisome-associated NPQ mechanism (9). Here, we show that the OCP is a photoactive protein sensing light intensity. Light induces the conversion between a dark stable orange form (OCP^o) and a metastable stable red form (OCP^r). The accumulation of the OCP^r is essential for the induction of the photoprotective mechanism. The OCP^r is present in whole cells under illuminations inducing the NPQ mechanism. Moreover, high intensities of blue-green light induced almost no fluorescence quenching in an OCP mutant in which the OCP photoconvertion was nearly abolished. The OCP^o to OCP^r conversion occurs with a very low quantum yield (≈0.03); this is likely to be because the OCP protein is involved in a photoprotective process that must be induced only under high light conditions. Moreover, the ratio of the two forms

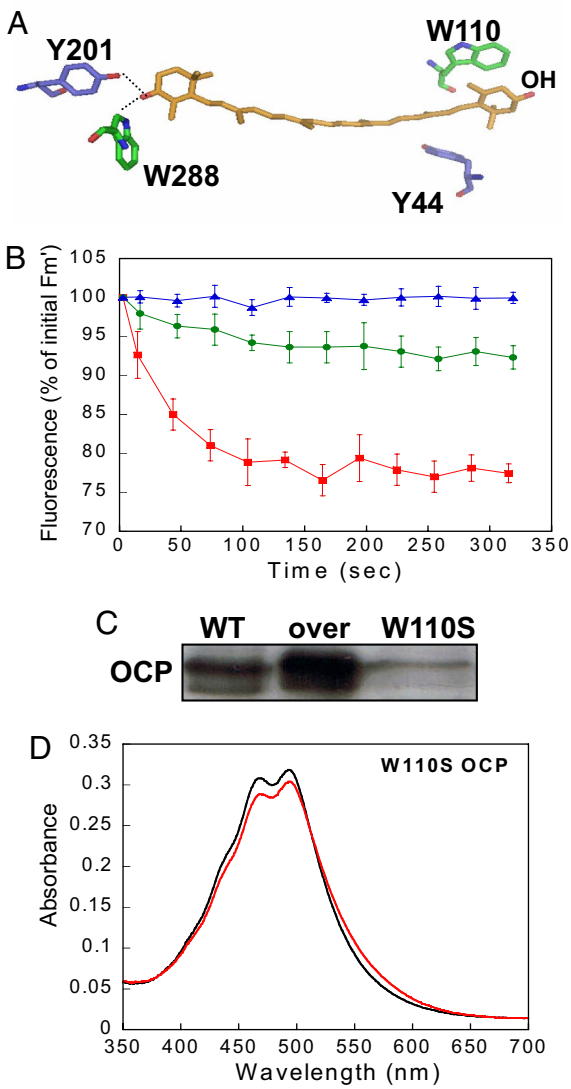

Fig. 3. The OCP^r is essential for the induction of the photoprotective mechanism. (*A*) Shown is 100% conserved Tyr and Trp interacting with the carotenoid. (*B*) Decrease of Fm′ during exposure of WT (red squares), overexpressing W110S OCP mutant (green circles), and His-tagged W110S OCP resistant mutant (blue triangles) cells to 740-μmol photons m^{-2} s^{-1} of blue-green light (400–550 nm). (*C*) Immunoblot detection in membrane-phycobilisome fractions from WT (*1*), overexpressing W110S OCP mutant (*2*), and His-tagged W110S OCP (*3*). Each lane contained 1.5-μg chlorophyll (*D*). Absorbance spectra of the dark orange form (OCP^o; black) and the light form (OCP^r; red). The OCP^o was illuminated during 15 min at 1,200-μmol photons m^{-2} s^{-1} and at 10°C.

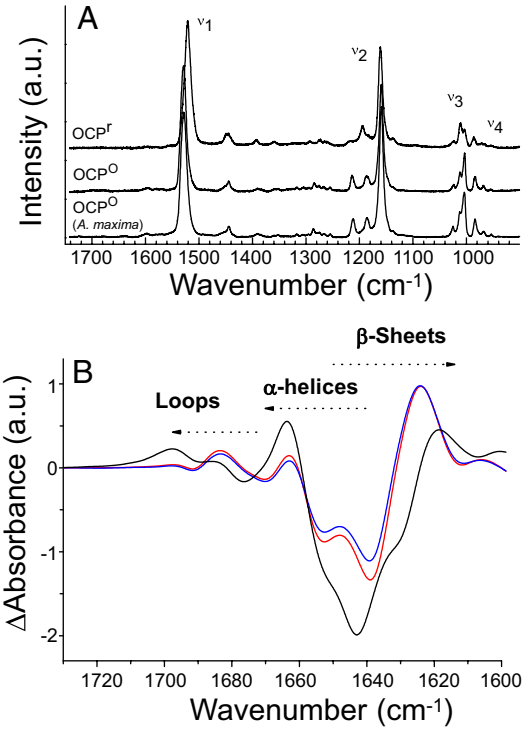

Fig. 4. Changes in the carotenoid and the protein upon illumination. (*A*) Resonance Raman spectra of *Synechocystis* PCC 6803 OCP^r and OCP^o and *Arthrospira maxima* OCP^o in the 1,740 to 820 cm^{-1} range and (*B*) light-minus-dark FTIR spectra of OCP in H_2O (black) and in D_2O ≈5 (red line) and 50 (blue line) seconds after illumination with a blue LED in the carbonyl region between 1,730 and 1,600 cm $^{-1}$ (Amide I region). The OCP^r minus OCP^o Amide I differential pattern is assigned to H-bond loosening (upshift) of the loops and α-helices carbonyl modes together with a H-bond strengthening (downshift of carbonyl modes) of the β-sheet.

under illumination depends on light intensity and temperature: more red active OCP^r at high light intensities and low temperatures. This provides a mechanism for the protein to sense photoinhibitory conditions: high light and light plus cold. Indeed, *in vivo*, greater fluorescence quenching is induced by increasing the light intensity and by lowering the temperature.

Retinal, a carotenoid derivative, is the chromophore of rhodopsins, a family of photoactive membrane-embedded proteins that are used throughout the animal and microbial kingdom as light receptors (25). Because retinal and hECN share structural similarities, it is worth considering whether OCP photoactivation could be similar to that of rhodopsin. However, our results suggest a completely different mechanism. Retinal is covalently bound to the protein by a protonated Schiff-base linkage to a Lys residue. The hECN in the OCP is close to an absolutely conserved Arg, but there is no covalent bond (19). Light induces an isomerisation of the retinal initiating the photocycle involving proton transfer between the Schiff-base and a carboxylate residue of the rhodopsin. In the OCP, no isomerisation was detected. Thus, although the specific changes in the carotenoid of OCP remain to be elucidated, they are clearly different from those occurring in retinal.

Light-driven structural changes in the carotenoid correlate with the protein conformational changes observed by FTIR; the structural rearrangement in the OCP may be a precondition for interaction with the phycobilisome or other proteins. Collectively, our data suggest a mechanism analogous to that of other blue-light responsive proteins, such as PYP and LOV domain-containing proteins. In each of these, blue light causes changes in the chromophore that induces disruption of hydrogen bonding networks and large conformational changes in the protein required for the light-responsive function (26, 27). By analogy, we posit that the absorption of blue light by the OCP alters the strength of one or both of the hydrogen bonds between the carotenoid and the protein. The resulting conformational changes in the protein could render the carotenoid more accessible and form a signal propagation pathway from the carotenoid to the surface of the OCP.

The C-terminal domain of the OCP (between residues 196 to 296) is structurally similar to the 7.8 kDa core linker protein (Noam Adir, personal communication; Fig. 6*A*), although lacking significant sequence homology. The linker protein consisting of a three-stranded β-sheet and one α-helix was cocrystallized

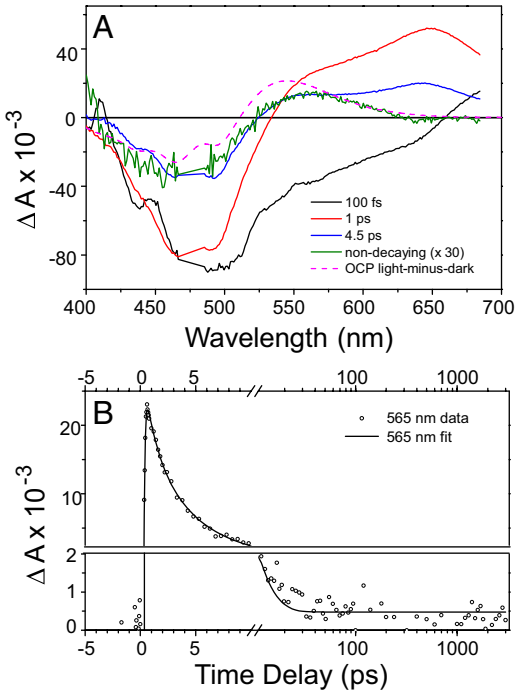

Fig. 5. Primary photochemistry of OCP revealed by femtosecond spectroscopy. OCP was excited with 50-fs flashes at 475 nm and the absorbance changes were monitored between 400 and 675 nm at time delays up to 3 ns. (*A*) Global analysis of time resolved data in the form of Evolution-Associated Difference Spectra (EADS). Four kinetic components with time constant of 100 fs (black), 1 ps (red), 4.5 ps (blue), and a long-lived component (green, expanded 30×). (*B*) Kinetic trace recorded at 565 nm (*symbols*) and the result of the global analysis (solid line). After decay of carotenoid excited-state signals on the picosecond timescale, a nondecaying photoproduct is formed at low yield. Note that the time axis is linear up to 10 ps and logarithmic thereafter. The vertical axis is split into two linear axes to show the long-lived product.

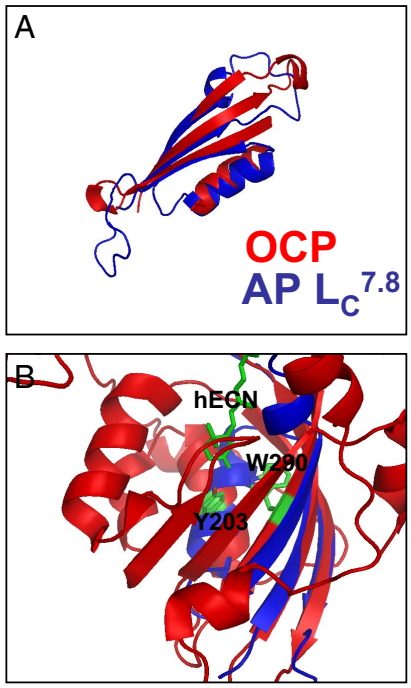

Fig. 6. Structural similarity between the OCP C-terminal domain and the core linker protein APL_C $^{7.8}$. (*A*) Superposition of the three strand β-sheet and the α-helix of the linker protein (blue) and of the C-terminal domain of the OCP (red). (*B*) The OCP C-terminal domain (red) showing the carotenoid and the Y203 and W290 residues (green stick representation) superimposed onto the linker protein structure (blue).

with allophycocyanin (APC) trimers that constitute part of the core of the phycobilisome (28). The structure revealed that the linker protein is bound within the central aperture of the APC trimer and directly interacts with the β84 chromophores of two APC subunits. Therefore, we hypothesize that the C-terminal OCP domain, by interacting with the center of an APC trimer, may bring the carotenoid into proximity of the APC chromophores. In addition, the Trp-290 and Tyr-203 residues, which interact with the carbonyl of the carotenoid, belong to the central strand of the β-sheet and to the α-helix of the C-terminal domain, respectively (Fig. 6*B*). Modifications in this domain caused by light-induced carotenoid changes could then possibly regulate the interaction between the carotenoid and the APC chromophores

Carotenoid molecules are able to quench excitation energy from tetrapyrrole molecules *in vitro* through energy transfer to their optically forbidden S_1 state, coupled to an intramolecular charge-transfer state (29). It was recently proposed that this mechanism is at the origin of the NPQ process in higher plants (7). Hydroxyechinenone, which contains a conjugated carbonyl group, clearly exhibits such an intramolecular charge transfer state (20). Therefore, we hypothesize that the OCP is not only the sensor of light but also the fluorescence quencher. Absorption of light by the hECN induces conformational changes of the carotenoid, shifting the absorption spectra toward the red region of the visible spectrum. The red shift is likely necessary to tune the optically forbidden S_1 state of hECN to a position to allow the energy transfer from the phycobilisome to the OCP. This mechanism is reminiscent of the gear-shift mechanism proposed to explain the role of zeaxanthin in higher plant NPQ (30). Possibly, an increase of charge-transfer character of the hECN excited states upon formation of OCP^r plays a role as well.

Although the molecular mechanism of the orange to red conversion and the exact role of the OCP in the cyanobacterial photoprotective mechanism await elucidation, our results suggest several mechanistic hypotheses that open an unexplored frontier in research on the functions of carotenoids: this is a unique report of a carotenoid protein functioning as a photoactive protein sensing light intensity.

Materials and Methods

His-Tagged Strains Construction. The *Synechocystis* PCC 6803 genome region containing the *slr1963* and *slr1964* genes was cloned. Then, the *slr1964* gene was interrupted by a kanamycin-resistance or a spectinomycin-resistance cassette and nucleotides encoding for 6 His were added in the *slr1963* gene. *Synechocystis* 6803 WT cells were transformed by these plasmids (see Fig. S2 *A*). To obtain a strain overexpressing the OCP, the genome region containing the *slr1963* and *slr1964* genes was cloned in the pPSBA2 ampicillin-resistant vector (31). Nucleotides encoding for 6 His were added in the 3′ side of the *slr1963* gene and a 1.3-kb kanamycin resistance gene was inserted. The plasmid obtained was used to transform the WT and the Cter6HSp/Sm mutant (see Fig. S2*B*). The point mutation (W to S) was added in the *slr1963* gene in the normally-expressing and overexpressing plasmids by site-directed mutagenesis. More details can be found in *SI Materials and Methods*.

Purification of the Orange Carotenoid Protein. In this study, we used OCP isolated from the K_m-resistant and Sp-resistant His-tagged OCP mutants. His-tagged OCP mutant cells (1-mg chl.ml^{-1}) in 0.1-M Tris·HCl pH = 8 buffer were broken in mild light using a French Press. The membranes were pelleted and the supernatant was loaded on a column of Ni-ProBond resin. The OCP was further purified on a Whatman DE-52 cellulose column. To quantify the OCP present in the different strains, membrane-phycobilisome fractions were isolated (10) and were analyzed by SDS page on 12%/2M urea in a Tris/Mes system (32). The OCP was detected by a polyclonal antibody against OCP (10). Carotenoids were extracted as previously

PLANT BIOLOGY

described (20) and separated by HPLC. Mass analysis was realized. More details can be found in *SI Materials and Methods*.

Spectroscopy Measurements. The kinetics of fluorescence changes were monitored in a modulated fluorometer (PAM) as previously described (8).

Transient absorption spectroscopy used 475-nm 50-fs laser pulses at 1 kHerz and energy per pulse of ≈200 nj. The data were subjected to global and target analysis (33) (see also *SI Materials and Methods*).

FTIR samples of the OCP in H_2O and D_2O were made with ≈2 μl of 5-mM OCP spread between two tightly fixed CaF_2 windows without any spacer. Light-minus-dark spectra were recorded using an FTIR spectrometer (IFS 66s Bruker) equipped with a nitrogen cooled photovoltaic mercury-cadmium-telluride detector (20 MHz, KV 100, Kolmar Technologies). A blue LED emitting at 470 nm was used for photoconversion.

Resonance Raman spectra, in resonance with the carotenoid electronic transitions, were recorded with a Jobin Yvon U1000 spectrometer equipped with liquid-nitrogen-cooled controlled-drift detector (Spectrum One, Jobin-Yvon). A coherent Argon laser (Innova 100) was used for excitation at 496.5 nm (OCP^o) or 528 nm (OCP^r). During spectral measurements, the temperature of the sample was maintained at 10 K to avoid photoconversion of OCP^o into OCP^r or relaxation of OCP^r into OCP^o. The dark form of OCP was flash frozen in a liquid nitrogen bath.

ACKNOWLEDGMENTS. We thank G. Ajlani and W. Vermaas for the gift of the plasmid pPSBA2 and D.W. Krogmann for stimulating discussions. We acknowledge Annie Marion-Poll, Jean-Pierre Boutin, and Lucien Kerhoas for discussions and advice about carotenoid analysis. This work was supported by grants from l'Agence Nationale de la Recherche, France (programs CAROPROTECT and BIOPHYSMEMBPROTS) (to A.W., D.K., A.G., and B.R.), and the INTRO2 European Union FP6 Marie Curie Research Training Network.

1. Horton P, Ruban AV, Walters RG (1996) Regulation of light harvesting in green plants. *Annu Rev Plant Physiol Plant Mol Biol* 47:655–684.
2. Niyogi K (1999) Photoprotection revisited: genetic and molecular approaches. *Annu Rev Plant Mol Biol* 50:333–359.
3. Demming-Adams B, Adams WW, III (2002) Antioxidants in photosynthesis and human nutrition. *Science* 298:2179–2153.
4. Holt N, Zigmantas D, Valkunas L, Li X-P, Niyogi K, Fleming G (2005) Carotenoid cation formation and the regulation of photosynthetic light harvesting. *Science* 307:433–436.
5. Standfuss J, *et al.* (2005) Mechanisms of photoprotection and non-photochemical quenching in pea light harvesting complex at 25Å resolution. *EMBO J* 24:919–928.
6. Pascal AA, *et al.* (2005) Molecular basis of photoprotection and control of photosynthetic light harvesting. *Nature* 436:134–137.
7. Ruban AV, *et al.* (2007) Identification of a mechanism of photoprotective energy dissipation in higher plants. *Nature* 450:575–578.
8. El Bissati K, Delphin E, Murata N, Etienne A-L, Kirilovsky D (2000) Photosystem II fluorescence quenching in the cyanobacterium *Synechocystis* PCC 6803: involvement of two different mechanisms. *Biochim Biophys Acta* 1457:229–242.
9. Wilson A, *et al.* (2006) A soluble carotenoid protein involved in phycobilisome-related energy dissipation in cyanobacteria. *Plant Cell* 18:992–1007.
10. Wilson A, Boulay C, Wilde A, Kerfeld C, Kirilovsky D (2007) Light induced energy dissipation in iron-starved cyanobacteria. Roles of OCP and IsiA proteins. *Plant Cell* 19:656–672.
11. Scott M, *et al.* (2006) Mechanism of the down regulation of photosynthesis by blue-light in the cyanobacterium *Synechocystis* PCC 6803. *Biochemistry* 45:8952–8958.
12. Rakhimberdieva M, Stadnichuk I, Elanskaya I, Karapetyan N (2004) Carotenoid-induced quenching of the phycobilisome fluorescence in photosystem II-deficient mutant of *Synechocystis* sp. *FEBS Lett* 574:85–88.
13. Rakhimberdieva M, Vavilin D, Vermaas W, Elanskaya I, Karapetyan N (2007) Phycobilin/chlorophyll excitation equilibration upon carotenoid-induced non-photochemical fluorescence quenching in phycobilisomes of the cyanobacterium *Synechocystis* sp PCC 6803. *Biochim Biophys Acta* 1767:757–765.
14. Rakhimberdieva M, Bolychevtseva Y, Elanskaya I, Karapetyan N (2007) Protein-protein interactions in carotenoid triggered quenching of phycobilisome fluorescence in *Synechocystis* sp PCC 6803. *FEBS Lett* 581:2429–2433.
15. Holt TK, Krogmann DW (1981) A carotenoid protein from cyanobacteria. *Biochim Biophys Acta* 637:408–414.
16. Wu YP, Krogmann DW (1997) The orange carotenoid protein of *Synechocystis* PCC 6803. *Biochim Biophys Acta* 1322:1–7.
17. Kerfeld C (2004) Water-soluble carotenoid proteins of cyanobacteria. *Arch Biochem Biophys* 430:2–9.
18. Kerfeld C (2004) Structure and function of the water-soluble carotenoid-binding proteins in cyanobacteria. *Photosynth Res* 81:b215–b225.
19. Kerfeld C, *et al.* (2003) The crystal structure of a cyanobacterial water-soluble protein. *Structure* 11:1–20.
20. Polivka T, Kerfeld CA, Pascher T, Sundström V (2005) Spectroscopic properties of the carotenoid 3′-hydroxyechinenone in the orange carotenoid protein from the cyanobacterium *Arthrospira maxima*. *Biochemistry* 44:3994–4003.
21. Robert B, Horton P, Pascal A, Ruban A (2004) Insights into the molecular dynamics of plant light-harvesting proteins in vivo. *Trends Plants Sci* 9:385–390.
22. Rimai L, Heyde ME, Gill D (1973) Vibrational spectra of some carotenoids and related linear polyenes. A raman spectroscopy study. *J Am Chem Soc* 95:4493–4501.
23. Krimm S, Bandekar J (1986) Vibrational spectroscopy and conformation of peptides, polypeptides, and proteins. *Adv Protein Chem* 38:181–364.
24. Iwata T *et al.* (2003) Light-induced structural changes in the LOV2 domain of *Adiantum* Phytochrome 3 studied by low-temperature FTIR and UV-visible spectroscopy. *Biochemistry* 42:8183–8191.
25. Spudich JL, Yang C-H, Jung K-H, Spudich EN (2000) Retinylidene proteins: structures and functions from archaea to humans. *Ann Rev Cell Dev Biol* 16:365–392.
26. Rubinstenn G, *et al.* (1998) Structural and dynamic changes of photoactive yellow protein during its photocycle in solution. *Nature Struct Biol* 5:568–570.
27. Harper S, Neil L, Gardner K (2003) Structural basis of a phototropin light switch. *Science* 301:1541–1544.
28. Reuter W, Wiegand G, Huber R, Than ME (1999) Structural analysis at 22 A of orthorhombic crystals presents the asymmetry of allophycocyanin-linker complex, $APL_C^{7.8}$, from phycobilisomes of Mastigocladus laminosus *Proc Natl Acad Sci USA* 96:1363–1368.
29. Berera R, *et al.* (2006) A simple artificial light-harvesting dyad as a model for excess energy dissipation in oxygenic photosynthesis. *Proc Natl Acad Sci USA* 103:5343–5348.
30. Frank HA, Bautista JA, Josue JS, Young AJ (2000) Mechanism of nonphotochemical quenching in green plants: Energies of the lowest excited singlet states of violaxanthin and zeaxanthin. *Biochemistry* 39:2831–2837.
31. Lagarde D, Beuf L, Vermaas W (2000) Increased production of zeaxanthin and other pigments by application of genetic engineering techniques to *Synechocystis* sp strain PCC 6803. *Appl Environ Microbiol* 66:64–72.
32. Kashino Y, Koike K, Satoh K (2001) An improved SDS-PAGE system for the analysis of membrane protein complexes. *Electrophoresis* 22:1004–1007.
33. van Stokkum IHM, Larsen DS, van Gondrelle R (2004) Global and target analysis of time-resolved spectra. *Biochim Biophys Acta* 1657:82–104.